Molecular Vision 2015; 21:324-334 <http://www.molvis.org/molvis/v21/324>
Received 23 October 2014 | Accepted 27 March 2015 | Published 30 March 2015

© 2015 Molecular Vision

MiRNA-21 promotes fibrosis in orbital fibroblasts from thyroid-associated ophthalmopathy

Tong Bo-ding, Xiao Man-Yi, Zeng Jie-Xi, Xiong Wei

Department of Ophthalmology and Eye Research Center, Hunan, China

Purpose: This study aimed to determine the role of miR-21 in orbital fibroblasts obtained from donors with thyroid-associated ophthalmopathy (TAO) and to elucidate the regulation of fibrosis by miR-21 in the pathological process of TAO.
Methods: The expression of miR-21 was investigated in orbital tissues from 26 donors with TAO and 10 donors without TAO. Human orbital fibroblasts were cultivated from TAO donors, and the role of miR-21 in orbital fibroblast proliferation, apoptosis, and differentiation was analyzed. Moreover, the effect of transforming growth factor-beta1 (TGF-β1) on miR-21 expression was also analyzed. In addition, the regulation of miR-21 in TGF-β1-induced collagen production was determined.
Results: The expression of miR-21 in orbital fibroblasts from TAO was higher than in donors without TAO. Additional experiments demonstrated that miR-21 enhanced proliferation, decreased apoptosis, and promoted differentiation in TAO orbital fibroblasts. Moreover, this study also showed that TGF-β1 induced miR-21 expression in a time- and dose-dependent manner and miR-21 promoted collagen I mRNA expression and total collagen production induced by TGF-β1. Additionally, miR-21 activated the TGF-β1/Smad signaling pathway by enhancing Smad3 phosphorylation.
Conclusions: The present study shows that miR-21 regulates cell proliferation, apoptosis, and differentiation in orbital fibroblasts from TAO, and acts as a mediator in TGF-β1-induced collagen production. These data predict a close association between miR-21 and orbital muscle fibrosis, and provide a novel therapeutic target for TAO.

Thyroid-associated ophthalmopathy (TAO), an autoimmune component of Graves' disease [1], is characterized by expanded volume of the orbital tissues, such as orbital fatty tissue and extraocular muscles (EOMs), in the limited space of the bony orbit [2]. EOMs and orbital connective tissues are expanded due to inflammatory cell infiltration, extracellular matrix protein accumulation, fibroblast proliferation, and increased amounts of orbital fatty tissue [3]. In fact, the EOMs are the major site of the disease process in TAO [4], since enlargement of the EOMs leads to orbital tissue fibrosis. Fibrosis is defined as overgrowth, hardening, or scarring of tissues, and is attributed to excess deposition of extracellular matrix (ECM) components, especially collagens [5,6]. Although many studies have focused on the pathological process of fibrosis in TAO, the actual mechanism has not been completely elucidated. In this regard, further study is needed to explore the mechanism involved in the process of orbital fibrosis in TAO.

MicroRNAs (miRNAs) are a class of 21- to 25-nucleotide single-stranded non-coding RNAs that regulate gene expression through binding to the mRNA 3′ untranslated region, leading to translational repression or mRNA degradation [7]. To date, hundreds of miRNA genes have been found in diverse animals, and many are phylogenetically conserved. Multiple roles of miRNA have been identified in development, cell death, cell proliferation, hematopoiesis, and patterning of the nervous system [8]. MiR-21 (accession number: MIMAT0000076) is a small multifaceted RNA involved in several physiologic processes [9]. MiR-21 has attracted the attention of researchers in various fields, such as development, oncology, stem cell biology, and aging, and has become one of the most studied miRNAs. MiR-21 is highly expressed in cancer cells and other lesions. It is a diagnostic and prognostic marker and serves as a potential therapeutic target in several diseases [9].

TGF-β is a key pathological mediator involved in the progression of fibrosis [10]. Increasing evidence shows that TGF-β may act by regulating miRNAs to exert its biologic effects, such as promoting fibrosis. For example, TGF-β induces collagen expression and renal fibrosis by suppressing miR-29 expression [11]. TGF-β also induces miR-192 expression and drives renal fibrosis [12]. TGF-β enhances miR-21 expression and mediates fibrogenic activation of pulmonary fibroblasts and lung fibrosis [13]. TGF-β also upregulates miR-21 expression in renal tissue, and thus promotes renal fibrosis [14].

Correspondence to: Xiong Wei: Department of Ophthalmology and Eye Research Center, The Second Xiangya Hospital, Central South University, 139 Ren-min Road, Changsha, Hunan, China; Phone: +86-13808469035; FAX: +86-0731-85294061; email: xiongweihn@126.com

MiRNA precursor molecules (miRNA mimics) are small, chemically modified double-stranded RNA molecules designed to mimic endogenous mature miRNAs, which enable miRNA functional analysis by the upregulation of miRNA activity. Anti-miRNA inhibitors are chemically modified, single-stranded nucleic acids designed to specifically bind to and inhibit endogenous miRNA molecules, which enable loss-of-function experiments through a decrease in miRNA activity. In this study, miRNA mimics and anti-miRNA inhibitors were used to investigate the function of miR-21 in orbital fibroblast fibrosis in TAO by up- or downregulating miRNA activity. To the best of our knowledge, this study is the first to evaluate the fibrotic effects of miR-21 in orbital fibroblasts in TAO.

METHODS

Specimens and cell lines: Fresh osteosarcoma tissue specimens were collected from 26 patients with TAO undergoing surgery at our hospital between December 2013 and March 2014. In addition, tissue specimens from ten patients undergoing routine non-thyroid-related strabismus surgery were collected as the control group. The specimens were preserved in liquid nitrogen immediately for subsequent testing. All research in human subjects adhered to the tenets of the Declaration of Helsinki, and the study protocol was approved by the Second Xiangya Hospital's Committee for the Protection of Human Subjects. Informed consent was obtained for each human subject.

Orbital fibroblast isolation and culture: Human orbital fibroblasts were cultivated from orbital fatty connective tissue obtained as surgical waste during decompression surgery for severe TAO (n=26) or during orbital surgery to resolve non-inflammatory conditions (n=10); the procedure was performed according to a previous report [15]. Tissue specimens were chopped mechanically and placed in Dulbecco's modified Eagle medium (DMEM; Gibco, Carlsbad, CA) containing 10% fetal bovine serum (FBS), glutamine (435 mg/ml), and 1% penicillin/streptomycin. The chopped tissues were allowed to attach to the bottom of the culture plates, and the cultures were maintained in a 37 °C, 5% CO_2, humidified environment. The medium was changed routinely every 3–4 days. The explants were removed when the fibroblasts were outgrown. The fibroblast monolayer was digested with trypsin/EDTA, and the cells were harvested after digestion and replated. Cells at passages 3–6 were used for the subsequent experiments.

Real-time PCR: Total RNA was extracted from the cells using the RNAiso Plus kit (Roche Diagnostics, Mannheim, Germany) according to the manufacturer's instructions. The expression of mature microRNAs was determined with TaqMan quantitative real-time PCR using the miRNA qPCR detection kit (GeneCopoeia, Rockville, MD) and normalized using the $2^{-\Delta\Delta}$ CT method [16] relative to small nuclear RNA U6 (U6 snRNA). The mRNA levels of α-smooth muscle actin (α-SMA) and collagen I were quantified with SYBR-Green quantitative real-time PCR detection kit and normalized to glyceraldehyde-3-phosphate dehydrogenase (GAPDH). The following PCR primers were used: α-SMA, 5′-GTC CAC CGC AAA TGC TTC TAA-3′ (forward) and 5′-AAA ACA CAT TAA CGA GTC AG-3′ (reverse) and an annealing temperature of 53 °C [17]; collagen I, 5′-AGT GGT TAC TAC TGG ATT GAC C-3′ (forward) and 5′-TTG CCA GTC TCC TCA TCC-3′ (reverse) [18] at an annealing temperature of 55 °C; and GAPDH, 5′-AAT CCC ATC ACC ATC TTC C-3′ (forward) and 5′-GAG TCC TTC CAC GAT ACC AA-3′ (reverse) at an annealing temperature of 54 ºC. The PCR procedure was as follows: polymerase activation for 4 min at 95 ºC, 40 cycles of amplification each consisting of 95 ºC for 5 s, 54 ºC for 20 s, and 72 ºC for 30 s. All PCRs were performed in triplicate.

Western blot: Orbital fibroblasts (5×10^5/well) were seeded in six-well plates, and the proteins from the cells were extracted using RIPA lysis buffer (Beyotime, Nantong, China). For western blotting, equal amounts of proteins were separated with sodium dodecyl sulfate–polyacrylamide gel electrophoresis (SDS–PAGE) and blotted onto a prewetted nitrocellulose membrane (GE Healthcare, Munich, Germany), followed by blocking of the membranes in 10% defatted milk in 0.2 M phosphate buffer saline (PBS; 1X; 32 mM NaH_2PO_4, 168 mM Na_2HPO_4, pH=7.5) at 4 °C for 4 h. The membranes were then probed with different primary antibodies. The following primary antibodies were used: mouse anti-ki67 (1:1,000), anti-Bcl-2 (1:1,000), anti-Bax (1:1,000), anti-α-SMA (1:1,000), anti-p-Smad3 (1:1,000), anti-Smad3 (1:1,000), and anti-β-actin monoclonal antibody (1:1,000; Santa Cruz Biotechnology, Santa Cruz, CA). After extensive washing with Tris Buffered Saline Tween-20 (TBST; 25 mM Tris, 150 mM NaCl, 0.05% Tween-20, pH=7.5), the membranes were incubated for 1 h at 25 °C with horseradish peroxidase (HRP)-conjugated secondary antibody (1:2,000; KangChen Bio-tech, Shanghai, China). Specific bands were visualized using enhanced chemiluminescence (ECL) reagent (Beyotime). Luminance was scanned using a Typhoon scanner (Amersham Biosciences, Piscataway, NJ). All experiments were performed in triplicate.

Transfection of miRNAs and siRNA: The oligonucleotide of anti-miR-21 and the negative control were designed according to a previous report [19] and synthesized by Shanghai

Genechem Co., Ltd. The miR-21 mimic and scrambled control microRNA were obtained from Bioneer Trade (Shanghai) Co., Ltd. For transfection, cells were seeded in 24-well plates and grown in antibiotic-free medium overnight until 30–50% confluence. After washing, about 0.4 nmol of microRNAs were mixed with 15 µl of Lipofectamine 2000 transfection reagent (Invitrogen, Carlsbad, CA), and the cells were maintained in a 37 °C, 5% CO_2 incubator for 6 h. The medium was replaced after 48 h, and the expression of miR-21 was confirmed with quantitative PCR.

TGF-β siRNA and negative-control siRNA were purchased from Santa Cruz Biotechnology. About 5×10^4 cells were seeded in 24-well plates. After growing for 24 h to reach 60–65% confluence, the cells were incubated with a mixture of siRNA and Lipofectamine 2000 reagent in 100 µl of serum-free Opti-MEM (Invitrogen) according to the manufacturer's instructions. The transfection efficiency was detected with real-time PCR and western blotting.

TGF-β1 treatment: Orbital fibroblasts were seeded at 5×10^3 cells per well in 96-well plates. For the time-dependent TGF-β1 treatment, the medium was replaced with fresh DMEM containing 0.5% PBS with or without 2 ng/ml human TGF-β1 (R&D Systems, Minneapolis, MN) for 0, 6, 12, 24, 48, and 72 h. For the dose-dependent TGF-β1 treatment, the medium was replaced with fresh DMEM containing 0, 0.5, 1, 2, 4, and 8 ng/ml TGF-β1 after 24 h.

Cell proliferation: Cell proliferation was determined with the 3-(4,5-dimethylthiazol-2-yl)-2,5-diphenyltetrazolium bromide (MTT) assay according to a previous report [20]. Briefly, 5×10^3 cells were seeded in 96-well plates and washed twice with PBS, and then 10 µl of MTT (5 mg/ml) was added to each well and incubated 37 °C for 6 h. The supernatant was replaced with 200 µl of isopropanol to dissolve the formazan crystals. Absorbance was measured at 560 nm with a Spectra Max Paradigm Multi-Mode Reader (Molecular Devices, Sydney, Austria). All experiments were performed in triplicate, and the results are presented as the percentage of control.

Cell apoptosis: To quantitatively evaluate the rate of apoptosis, Annexin V-propidium iodide (AV-PI) staining was performed. Briefly, after pretreatment with the caspase inhibitor z-VAD-fmk, transfected cells were harvested and washed three times with PBS. Then, cells were centrifuged for 10 min, followed by suspension in 500 µl of binding buffer including 5 µl of fluorescein isothiocyanate (FITC)-conjugated Annexin V. Following incubation for 10 min in the dark, 5 µl of propidium iodide (PI) was added. Ultimately, all specimens were assessed by flow cytometry with a FACS-Calibur using CellQuest software (Becton Dickinson, San Jose, CA). The results are shown as a percentage of the total cells counted.

Measurement of collagen content: The total collagen content was measured using the Sircol collagen assay kit (Biocolor Lifescience, Belfast, England) according to the manufacturer's instructions. Briefly, 5×10^3 cells were seeded in 96-well plates and then incubated for 24 h at 4 °C with stirring. After centrifugation, 100 µl of the supernatant of each well was transferred to 1.5 ml centrifuge tubes and used for the assay. To each tube, 1.0 ml of Sircol dye reagent was added. The tubes were then placed on a gentle mechanical shaker for 30 min at 4 °C. Then, the tubes were centrifuged at 11,181 ×g for 10 min. After centrifugation, the pellet was suspended in 750 µl of ice-cold acid-salt wash reagent and centrifuged again. Then, 250 µl of alkali reagent was added to each well, and the tubes were placed on a gentle mechanical shaker. Finally, each sample (200 µl) was transferred to the individual wells of a 96-well plate and read at 540 nm with a spectrophotometer. The total collagen content was also determined by assaying the cell protein content.

Statistical analysis: Data are presented as mean ± standard deviation (SD) from a minimum of three experiments. Statistical analyses were performed using SPSS19.0 software (SPSS, Chicago, IL). Statistical significance was assessed with the Student *t* test. A p value <0.05 was considered statistically significant.

RESULTS

MiR-21 is highly expressed in human thyroid-related eye disease tissues: Expression of miR-21 is significantly upregulated in fibrotic-related disease and exerts a vital role in the progression of fibrosis. However, the related role of miR-21 in thyroid-related eye disease tissues remain poorly understood. We examined miR-21 expression in orbital fibroblasts from normal (n=10) or TAO (n=26) tissues. The results show that the expression levels of miR-21 were obviously higher in orbital fibroblasts from TAO tissues than those from the normal human eye tissues ($p<0.05$, Figure 1). Collectively, these results suggest dramatic upregulation of miR-21 in orbital fibroblasts from TAO donors.

MiR-21 promotes orbital fibroblast proliferation: To investigate the effect of miR-21 on the progression of fibrosis in TAO, we successfully downregulated the expression levels of miR-21 in TAO orbital fibroblasts by anti-miR-21 and upregulated levels by transfection with an miR-21 mimic, as detected with real-time PCR ($p<0.05$, Figure 2A). Additional MTT analysis confirmed that miR-21 inhibition by anti-miR-21 sharply decreased orbital fibroblast proliferation compared to the control. In contrast, overexpression of miR-21 by

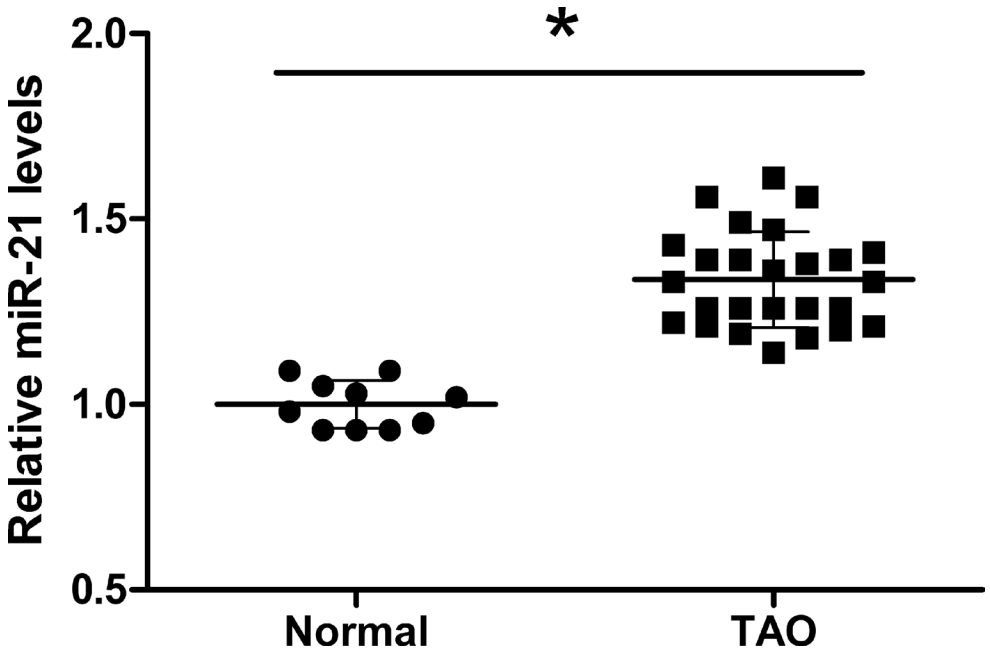

Figure 1. Expression of miR-21 in orbital fibroblasts from the eye tissue of normal subjects (n=10) or TAO donors (n=26). Results are expressed as mean ± standard deviation (SD; *p<0.05 versus control).

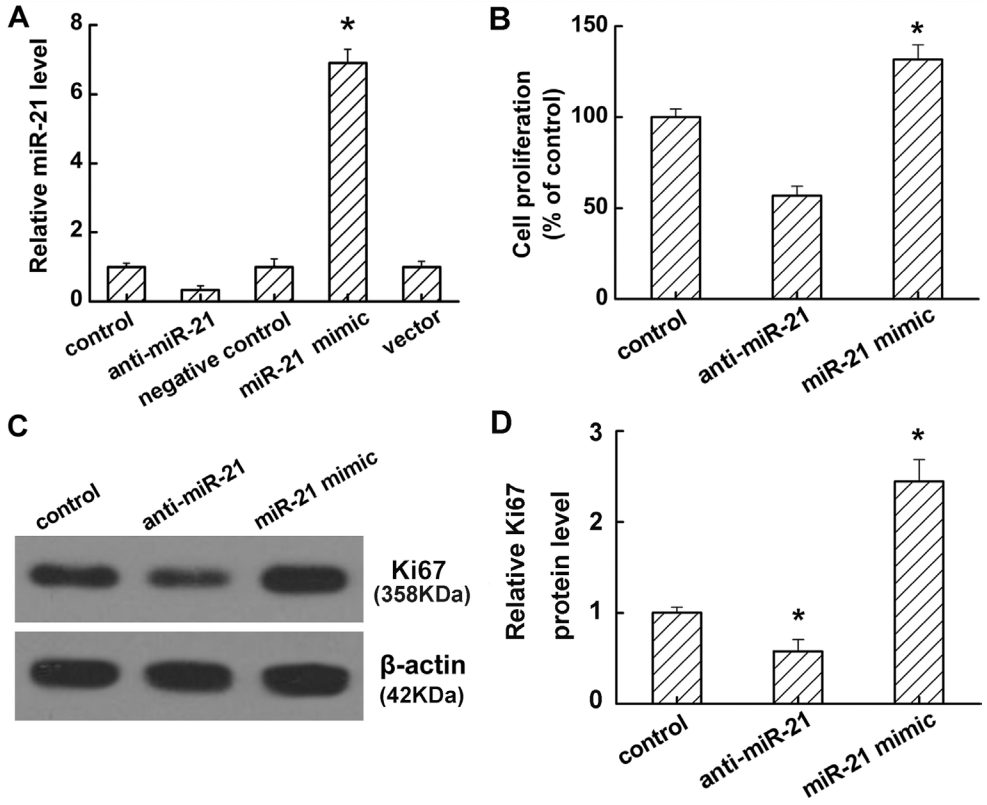

Figure 2. Effect of miR-21 on the proliferation of orbital fibroblasts from TAO donors (n=3). **A**: Real-time PCR shows miR-21 expression after different treatments. **B**: The proliferation of anti-miR-21 and miR-21 mimic transfected cells. **C**: Western blot analysis of the protein level of Ki67. **D**: Quantification of the protein band density in panel **C**. Results are expressed as mean ± standard deviation (SD; *p<0.05 versus control). Data are representative of three independent experiments.

mimic transfection aggregated the growth of orbital fibroblasts (p<0.05, Figure 2B). Moreover, anti-miR-21 treatment significantly inhibited Ki67 protein expression, whereas the miR-21 mimic obviously promoted Ki67 protein expression (p<0.05, Figure 2C,D).

MiR-21 inhibits orbital fibroblast apoptosis: To explore whether cell apoptosis is associated with orbital fibroblast growth promotion induced by miR-21, we assessed orbital fibroblast apoptosis with Annexin V-FITC and PI staining using flow cytometry. As shown in Figure 3A, after treatment with anti-miR-21, dramatic upregulation in the number of apoptotic cells was observed. In contrast, transfection with the miR-21 mimic obviously decreased the ratio of apoptotic cells (all p<0.05, Figure 3B). Furthermore, the induction of apoptosis was further manifested by the expression of Bcl-2 and Bax. Anti-miR-21 suppressed Bcl-2 whereas it induced Bax expression; conversely, miR-21 overexpression triggered a significant increase in Bcl-2 and decreased Bax protein expression (p<0.05, Figure 3C,D). These results indicate that miR-21 acts as an antiapoptosis factor in orbital fibroblasts.

MiR-21 promotes orbital fibroblast development: Fibroblast-to-myofibroblast differentiation is a critical process in the pathogenesis of several fibrotic diseases, including TAO. To determine whether miR-21 might affect this process, differentiation was induced with 2 ng/ml TGF-β1 for 24 h. Real-time PCR and western blot analysis demonstrated that the mRNA and protein levels of α-SMA, a biomarker of myofibroblast differentiation, were markedly downregulated by anti-miR-21 but upregulated by the miR-21 mimic (p<0.05, Figure 4). These results indicate that miR-21 may promote myofibroblast differentiation induced by TGF-β1.

Promotion of miR-21 expression by TGF-β in orbital fibroblasts: We next examined the influence of TGF-β1 on miR-21 levels in TAO orbital fibroblasts. Cells were treated with 2 ng/mL of TGF-β1 for 0, 6, 12, 24, 48, and 72 h, and miR-21 levels in culture media were analyzed with real-time PCR. The results show that TGF-β1, but not PBS, induced miR-21 expression in a time-dependent manner, with peak expression observed after 24 h of treatment (p<0.05, Figure 5A). Incubation of such cells for 24 h with a range of TGF-β1 concentrations (0.5–8 ng/mL) caused a dose-dependent increase in miR-21 (p<0.05, Figure 5B). Moreover, the induction of miR-21 expression by TGF-β1 was inhibited by TGF-β1 siRNA but not by control siRNA (p<0.05, Figure 5B).

MiR-21 promotes TGF-β-induced collagen production in orbital fibroblasts: To evaluate the effect of miR-21 on collagen production in TAO orbital fibroblasts, the total collagen content and mRNA levels of collagen I were measured after the TAO orbital fibroblasts were treated with or without 2 ng/ml TGF-β1 for 24 h. As shown in Figure 6, TGF-β1 treatment significantly increased the total collagen content and the mRNA level of collagen I; notably, the collagen I levels were sharply decreased when the cells treated with anti-miR-21 and enhanced by the miR-21 mimic (all p<0.05, Figure 6A,B).

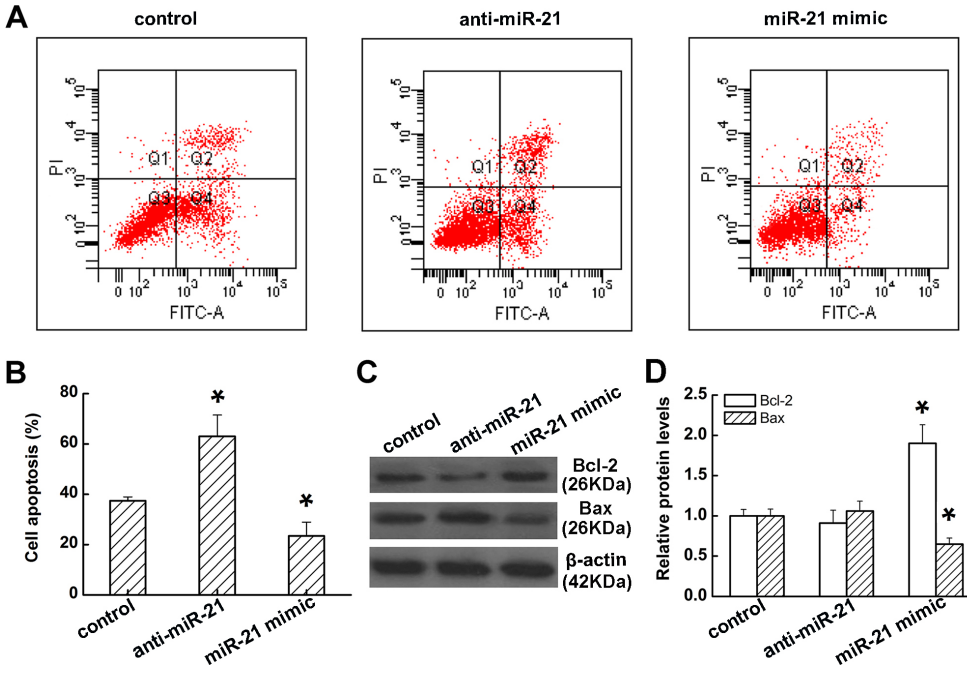

Figure 3. Effect of miR-21 on apoptosis in orbital fibroblasts from TAO donors (n=3). **A**: The effect of miR-21 on cell apoptosis. **B**: Quantification of the data in panel **A**. **C**: Western blot analysis of the protein level of Bcl-2 and Bax. **D**: Quantification of the protein band density in panel **C**. Results are expressed as mean ± standard deviation (SD; *p<0.05 versus control). Data are representative of three independent experiments.

MiR-21 activates TGF-β/Smad signaling by promoting Smad3 phosphorylation: To determine whether miR-21 plays a role in TGF-β/Smad signaling, we analyzed the phosphorylation levels of Smad3 in miR-21 upregulated and downregulated orbital fibroblasts. The results show that anti-miR-21 inhibited Smad3 phosphorylation; however, the miR-21 mimic significantly enhanced Smad3 phosphorylation (all $p<0.05$, Figure 7A,B), indicating that miR-21 overexpression might promote TGF-β/Smad activation.

DISCUSSION

The symptoms of TAO include cosmetic deficits, such as lid swelling, proptosis, and lid retraction, and functional deficits that manifest as limited ocular movement and visual impairment [6]. Fibroblast proliferation, extracellular matrix deposition, and adipocyte differentiation and proliferation lead to edema, enlargement of the extraocular muscles, and increased volume of the orbital soft tissues [21]. In turn, edema, inflammation, and late fibrosis account for the decreased function of the EOMs, despite relative preservation of the fibers themselves. Orbital fibroblasts are thought to be a key target and effector cell in the pathogenesis of TAO [4,22].

Numerous studies have demonstrated the effects of miR-21 in tumors, such as promoting tumor cell proliferation [23] and invasion [24] and inhibiting apoptosis [25]. Apart from this, increasing evidence suggests that miR-21 plays an indispensable role in the process of fibrosis in many diseases. For example, miR-21 mediates the fibrogenic activation of pulmonary fibroblasts in lung fibrosis [13], promotes renal fibrosis [14], accelerates atrial fibrosis, and promotes structural remodeling of the atrial myocardium [26]. Pulmonary artery stenosis causes significant myocardial remodeling and leads to impaired right ventricle function. Treatment with antagomir-21 reduces myocardial fibrosis and improves right ventricle function. miR-21 promotes myocardial fibrosis and impairs right ventricle function, and inhibition of miR-21 by a specific antagomir may offer a novel therapeutic option in right heart hypertrophy [27]. In this study, we found that the expression of miR-21 was higher in orbital fibroblasts from patients with TAO than those without TAO, indicating that miR-21 may be involved in the pathogenic progression of fibrosis in TAO. Orbital fibroblast proliferation, apoptosis, and differentiation are closely associated with EOM fibrosis in the pathological process of TAO. To elucidate the probable role of miR-21 in EOM fibrosis of TAO, we down- and

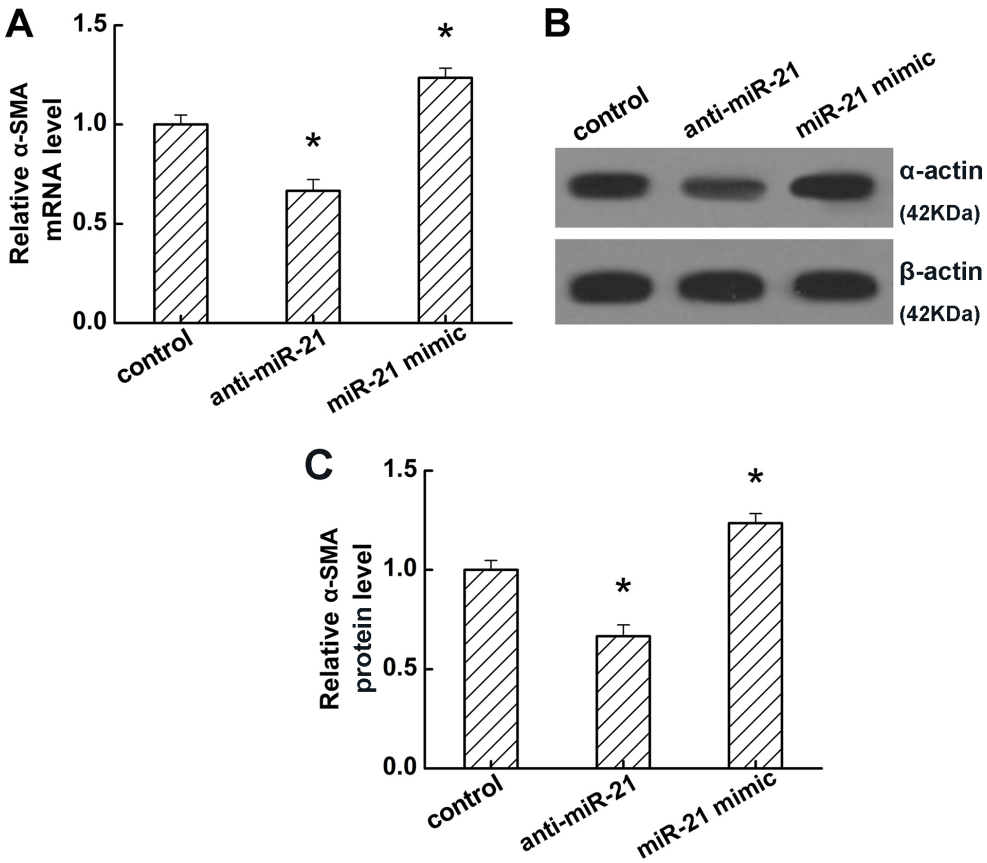

Figure 4. Effect of miR-21 on mRNA and protein expression of α-SMA in orbital fibroblasts from TAO donors (n=3). **A**: Real-time PCR analysis of the mRNA level of α-smooth muscle actin (α-SMA). **B**: Western blot analysis of the protein level of α-SMA. **C**: Quantification of the protein band density in panel **B**. Results are expressed as mean ± standard deviation (SD; *$p<0.05$ versus control). Data are representative of three independent experiments.

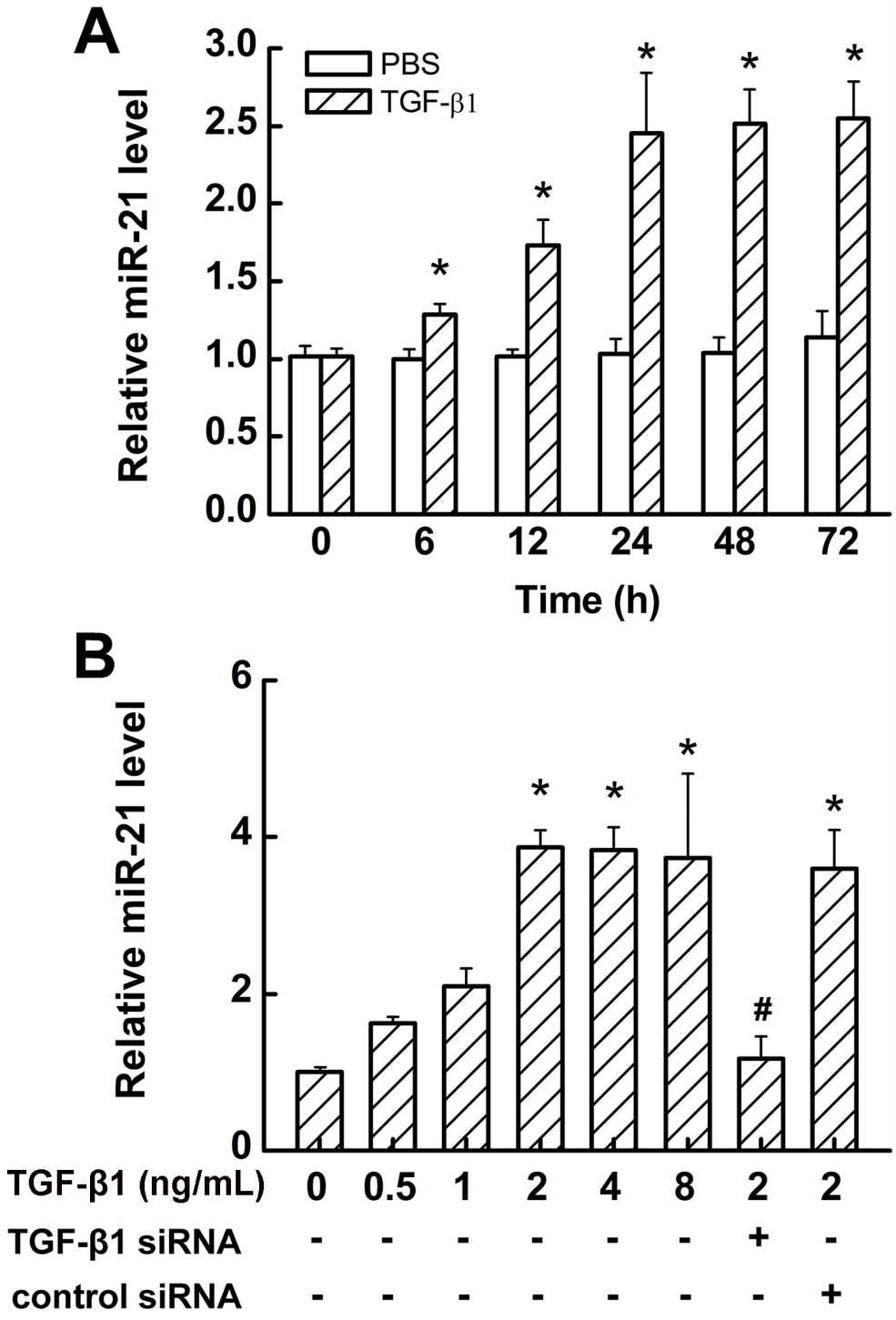

Figure 5. TGF-β1 induces miR-21 expression in a time- and dose-dependent manner in fibroblasts from TAO donors (n=3). **A**: Real-time PCR analysis showing that transforming growth factor-beta1 (TGF-β1; 2 ng/ml) induces miR-21 expression in a time-dependent manner. **B**: Real-time PCR analysis showing that TGF-β1 induces miR-21 expression after 24 h in a dose-dependent manner. Each bar represents the mean ± standard deviation (SD) of at least three independent experiments. (*p<0.05 versus control, #p<0.05, versus 2 ng/ml TGF-β1 treated control).

upregulated miR-21 levels in TAO orbital fibroblasts. The results show that miR-21 downregulation inhibited orbital fibroblast proliferation and differentiation, and promoted orbital fibroblasts apoptosis; however, miR-21 upregulation enhanced orbital fibroblast proliferation and differentiation, and blocked orbital fibroblast apoptosis.

TGF-β is a central pathological mediator involved in the progression of fibrosis [10]. TGF-β enhances miR-21 expression and mediates fibrosis in the lung [13] and kidney [14]. To work out the underlying mechanism of miR-21 in orbital muscle fibrosis, time- and dose-dependent TGF-β1 treatment was performed in orbital fibroblasts. Our data suggest that

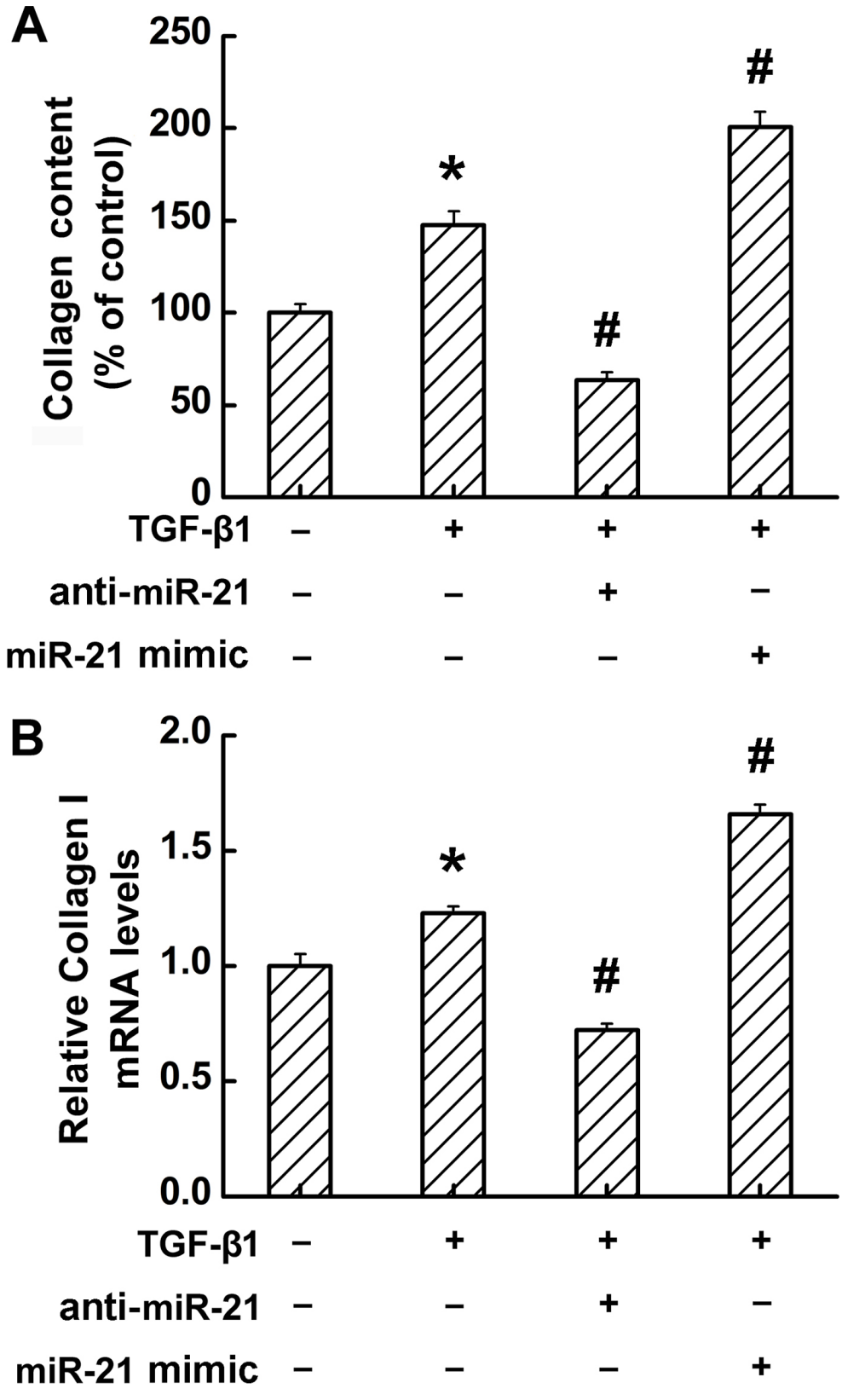

Figure 6. Effect of TGF-β1 and miR-21 on collagen production and mRNA expression in fibroblasts from TAO donors (n=3). Results are expressed as a percentage of untreated control values presented as mean ± standard deviation (SD; *p<0.05 versus transforming growth factor-beta1 (TGF-β) untreated control; #p<0.05 versus anti-miR-21-treated cells). Data are representative of three independent experiments.

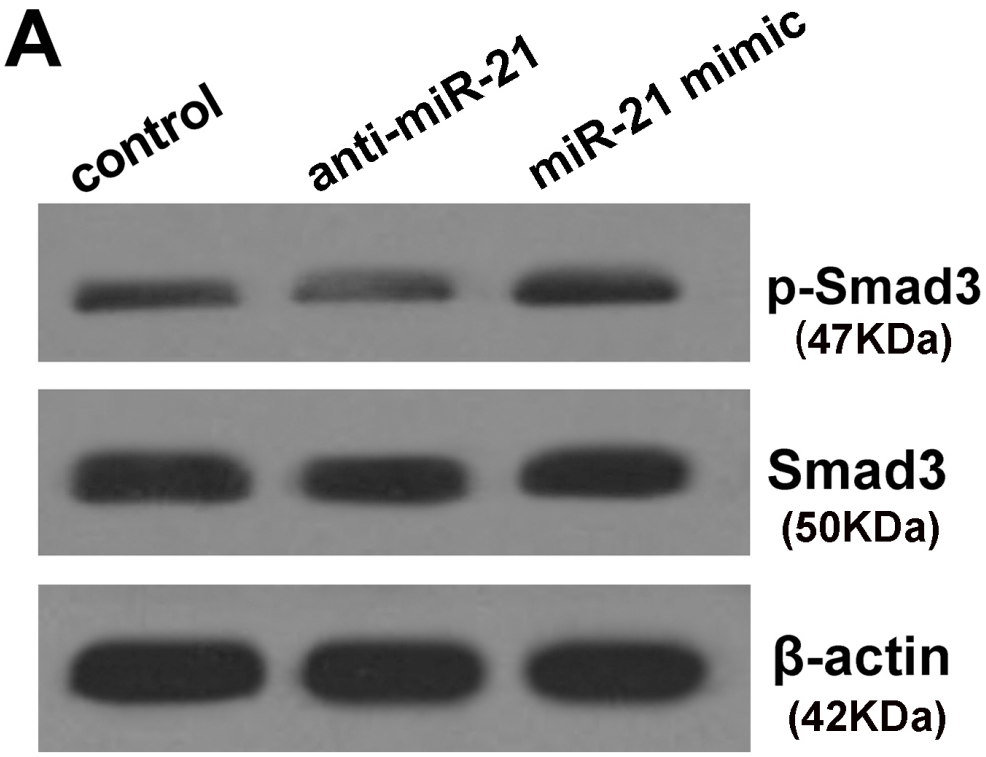

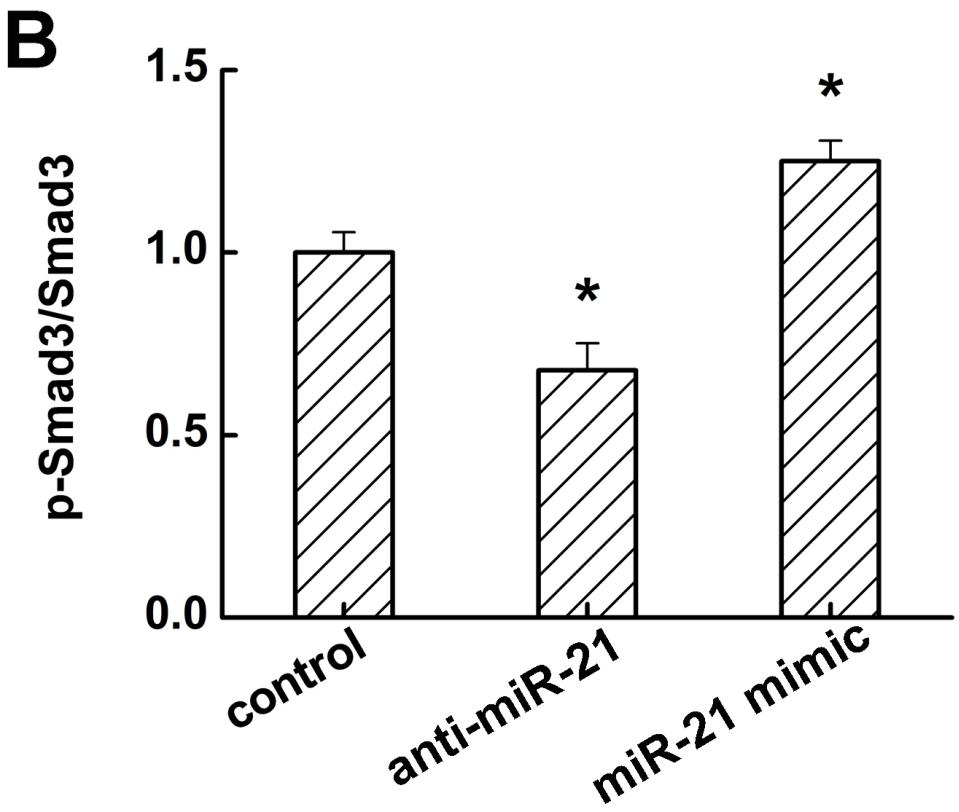

Figure 7. Effect of miR-21 on the phosphorylation of Smad3 in fibroblasts from TAO donors (n=3). Results are expressed as the percentage of untreated control values presented as mean ± standard deviation (SD; *p<0.05 versus control). Data are representative of three independent experiments.

TGF-β1 induced miR-21 expression in orbital fibroblasts in a time- and dose-dependent manner. Moreover, overexpression of miR-21 enhanced TGF-β1-induced total collagen I expression and the collagen I mRNA level, whereas inhibition of miR-21 by anti-miR-21 decreased the total collagen content and collagen I mRNA level in the context of TGF-β1 treatment. We also showed that anti-miR-21 blocked Smad3 phosphorylation; in contrast, the miR-21 mimic activated Smad3 phosphorylation. These results indicate that miR-21 mediates TGF-β/Smad signaling in the progression of orbital muscle fibrosis.

Taken together, the present study shows that miR-21 is upregulated in orbital fibroblasts from TAO, and further in vitro experiments demonstrated that miR-21 promotes orbital muscle fibrosis in TAO. This investigation provides evidence suggesting that inhibiting miR-21 expression might be a potential antifibrotic therapy in the treatment of TAO in the future. Additional in vivo experiments are needed to elucidate the exact function of miR-21 in TAO.

ACKNOWLEDGMENTS

Authors contribution: Tong Bo-ding was responsible for the design and overall performance of the study as well as data analysis and preparation of the manuscript. Xiao Man-yi and Zeng Jie-xi were involved in the design and conduct of this study. Ying-Hui Zhang, Ming-Wei Shao, Xiong Wei was responsible for the data collection and analysis. All authors read and approved the final manuscript.

REFERENCES

1. Burch HB, Lahiri S, Bahn RS, Barnes S. Superoxide radical production stimulates retroocular fibroblast proliferation in Graves' ophthalmopathy. Exp Eye Res 1997; 65:311-6. [PMID: 9268599].
2. Chung SA, Jeon BK, Choi Y-H, Back KO, Lee JB, Kook KH. Pirfenidone attenuates the IL-1β-induced hyaluronic acid increase in orbital fibroblasts from patients with thyroid-associated ophthalmopathy. Invest Ophthalmol Vis Sci 2014; 55:2276-83. [PMID: 24627146].
3. Lee W-M, Paik J-S, Cho W-K, Oh E-H, Lee S-B, Yang S-W. Rapamycin enhances TNF-α-induced secretion of IL-6 and IL-8 through suppressing PDCD4 degradation in orbital fibroblasts. Curr Eye Res 2013; 38:699-706. [PMID: 23281820].
4. Pappa A, Lawson JMM, Calder V, Fells P, Lightman S. T cells and fibroblasts in affected extraocular muscles in early and late thyroid associated ophthalmopathy. Br J Ophthalmol 2000; 84:517-22. [PMID: 10781517].
5. Wynn TA. Cellular and molecular mechanisms of fibrosis. J Pathol 2008; 214:199-210. [PMID: 18161745].
6. Kim H, Choi Y-H, Park SJ, Lee SY, Kim SJ, Jou I, Kook KH. Antifibrotic effect of Pirfenidone on orbital fibroblasts of patients with thyroid-associated ophthalmopathy by decreasing TIMP-1 and collagen levels. Invest Ophthalmol Vis Sci 2010; 51:3061-6. [PMID: 20053983].
7. Zavadil J, Narasimhan M, Blumenberg M, Schneider RJ. Transforming growth factor-beta and microRNA:mRNA regulatory networks in epithelial plasticity. Cells Tissues Organs 2007; 185:157-61. [PMID: 17587821].
8. Ambros V. The functions of animal microRNAs. Nature 2004; 431:350-5. [PMID: 15372042].
9. Krichevsky AM, Gabriely G. miR-21: a small multi-faceted RNA. J Cell Mol Med 2009; 13:39-53. [PMID: 19175699].
10. Leask A, Abraham DJ. TGF-β signaling and the fibrotic response. FASEB J 2004; 18:816-27. [PMID: 15117886].
11. Wang B, Komers R, Carew R, Winbanks CE, Xu B, Herman-Edelstein M, Koh P, Thomas M, Jandeleit-Dahm K, Gregorevic P. Suppression of microRNA-29 expression by TGF-β1 promotes collagen expression and renal fibrosis. J Am Soc Nephrol 2012; 23:252-65. [PMID: 22095944].
12. Chung AC, Huang XR, Meng X, Lan HY. miR-192 mediates TGF-β/Smad3-driven renal fibrosis. J Am Soc Nephrol 2010; 21:1317-25. [PMID: 20488955].
13. Liu G, Friggeri A, Yang Y, Milosevic J, Ding Q, Thannickal VJ, Kaminski N, Abraham E. miR-21 mediates fibrogenic activation of pulmonary fibroblasts and lung fibrosis. J Exp Med 2010; 207:1589-97. [PMID: 20643828].
14. Zhong X, Chung ACK, Chen H-Y, Meng X-M, Lan HY. Smad3-mediated upregulation of miR-21 promotes renal fibrosis. J Am Soc Nephrol 2011; 22:1668-81. [PMID: 21852586].
15. Cao HJ, Wang H-S, Zhang Y, Lin H-Y, Phipps RP, Smith TJ. Activation of human orbital fibroblasts through CD40 engagement results in a dramatic induction of hyaluronan synthesis and prostaglandin endoperoxide H synthase-2 expression: insight into potential PATHOGENIC MECHANISMS of thyroid-associated ophthalmopathy. J Biol Chem 1998; 273:29615-25. [PMID: 9792671].
16. Pfaffl MW. A new mathematical model for relative quantification in real-time RT–PCR. Nucleic Acids Res 2001; 29:e45-45. [PMID: 11328886].
17. Baouz S, Giron-Michel J, Azzarone B, Giuliani M, Cagnoni F, Olsson S, Testi R, Gabbiani G, Canonica GW. Lung myofibroblasts as targets of salmeterol and fluticasone propionate: inhibition of α-SMA and NF-κB. Int Immunol 2005; 17:1473-81. [PMID: 16210331].
18. Saed GM, Zhang W, Chegini N, Holmdahl L, Diamond MP. Alteration of type I and III collagen expression in human peritoneal mesothelial cells in response to hypoxia and transforming growth factor-β1. Wound Repair Regen 1999; 7:504-10. [PMID: 10633010].
19. Chen Y, Liu W, Chao T, Zhang Y, Yan X, Gong Y, Qiang B, Yuan J, Sun M, Peng X. MicroRNA-21 down-regulates the expression of tumor suppressor PDCD4 in human

glioblastoma cell T98G. Cancer Lett 2008; 272:197-205. [PMID: 19013014].

20. Song D, Wang R, Zhong Y, Li W, Li H, Dong F. Locally produced insulin-like growth factor-1 by orbital fibroblasts as implicative pathogenic factor rather than systemically circulated IGF-1 for patients with thyroid-associated ophthalmopathy. Graef Arch Clin Exp 2012; 250:433-40. [PMID: 22159761].

21. Hatton MP, Rubin P. The pathophysiology of thyroid-associated ophthalmopathy. Ophthalmol Clin 2002; 15:113-9. [PMID: 12064074].

22. Heufelder AE. Involvement of the orbital fibroblast and TSH receptor in the pathogenesis of Graves' ophthalmopathy. Thyroid 1995; 5:331-40. [PMID: 7488878].

23. Yao Q, Xu H, Zhang Q-Q, Zhou H, Qu L-H. MicroRNA-21 promotes cell proliferation and down-regulates the expression of programmed cell death 4 (PDCD4) in HeLa cervical carcinoma cells. Biochem Biophys Res Commun 2009; 388:539-42. [PMID: 19682430].

24. Hiyoshi Y, Kamohara H, Karashima R, Sato N, Imamura Y, Nagai Y, Yoshida N, Toyama E, Hayashi N, Watanabe M. MicroRNA-21 regulates the proliferation and invasion in esophageal squamous cell carcinoma. Clin Cancer Res 2009; 15:1915-22. [PMID: 19276261].

25. Chan JA, Krichevsky AM, Kosik KS. MicroRNA-21 is an antiapoptotic factor in human glioblastoma cells. Cancer Res 2005; 65:6029-33. [PMID: 16024602].

26. Adam O, Löhfelm B, Thum T, Gupta SK, Puhl S-L, Schäfers H-J, Böhm M, Laufs U. Role of miR-21 in the pathogenesis of atrial fibrosis. Basic Res Cardiol 2012; 107:1-12. [PMID: 22760500].

27. Neumann J, Janssen W, Kojonazarov B, Döbele C, Ghofrani H, Weissmann N, Grimminger F, Seeger W, Dimmeler S, Schermuly R. Role of microRNA-21 in right ventricular hypertrophy and fibrosis. Pneumologie 2012; 66:A701-.

Articles are provided courtesy of Emory University and the Zhongshan Ophthalmic Center, Sun Yat-sen University, P.R. China. The print version of this article was created on 30 March 2015. This reflects all typographical corrections and errata to the article through that date. Details of any changes may be found in the online version of the article.